Cell

A Cortical Circuit for Gain Control by Behavioral State

Yu Fu,[1,*] Jason M. Tucciarone,[2,3] J. Sebastian Espinosa,[1] Nengyin Sheng,[4] Daniel P. Darcy,[1] Roger A. Nicoll,[4] Z. Josh Huang,[2] and Michael P. Stryker[1,*]
[1]Center for Integrative Neuroscience, Department of Physiology, University of California, 675 Nelson Rising Road, San Francisco, CA 94158, USA
[2]Cold Spring Harbor Laboratory, 1 Bungtown Road, Cold Spring Harbor, NY 11724, USA
[3]MSTP/Neuroscience graduate Program, Stony Brook University, Stony Brook, NY 11790, USA
[4]Departments of Cellular and Molecular Pharmacology and Physiology, University of California, San Francisco, CA 94158, USA
*Correspondence: yufu@phy.ucsf.edu (Y.F.), stryker@phy.ucsf.edu (M.P.S.)
http://dx.doi.org/10.1016/j.cell.2014.01.050

SUMMARY

The brain's response to sensory input is strikingly modulated by behavioral state. Notably, the visual response of mouse primary visual cortex (V1) is enhanced by locomotion, a tractable and accessible example of a time-locked change in cortical state. The neural circuits that transmit behavioral state to sensory cortex to produce this modulation are unknown. In vivo calcium imaging of behaving animals revealed that locomotion activates vasoactive intestinal peptide (VIP)-positive neurons in mouse V1 independent of visual stimulation and largely through nicotinic inputs from basal forebrain. Optogenetic activation of VIP neurons increased V1 visual responses in stationary awake mice, artificially mimicking the effect of locomotion, and photolytic damage of VIP neurons abolished the enhancement of V1 responses by locomotion. These findings establish a cortical circuit for the enhancement of visual response by locomotion and provide a potential common circuit for the modulation of sensory processing by behavioral state.

INTRODUCTION

Sensory responses in neocortex are modulated by behavioral states, sleep and wakefulness being the states studied longest. Attention, for example, has long been known to alter the cortical response to sensory stimuli (Fontanini and Katz, 2008; Maunsell and Cook, 2002; Posner and Petersen, 1990). Recently, locomotion was found to increase the gain of excitatory neurons in mouse primary visual cortex (V1) without altering their spontaneous activity or orientation selectivity (Niell and Stryker, 2010). This increase was found to be central rather than peripheral because there was no similar increase in the lateral geniculate nucleus (LGN), which relays activity from the eyes to the cortex. The neural circuit that transmits information about behavioral state to sensory cortex is largely unknown. Previous studies have shown that different types of cortical neurons were differentially modulated by behavioral state (Reynolds and Chelazzi, 2004). In particular, some putative inhibitory neurons were modulated differently from the more typical broad-spiking excitatory neurons (Chen et al., 2008; Mitchell et al., 2007; Niell and Stryker, 2010). Changes in the balance between intrinsic excitatory and inhibitory conductances have long been linked to the change of brain state (Bazhenov et al., 2002; Hill and Tononi, 2005), and one salient feature of awake cortical responses is powerful inhibition (Haider et al., 2013). Inhibitory neurons may alter dendritic integration of sensory signals (Huber et al., 2012; Petreanu et al., 2012; Xu et al., 2012), and different inhibitory neurons have been hypothesized to play critical roles in behavioral state-dependent modulation of sensory processing (Buia and Tiesinga, 2008). However, electrophysiology alone does not allow one to distinguish among the large variety of GABAergic neurons with distinct physiological functions (Huang et al., 2007; Markram et al., 2004). Recent advances in mouse genetics and in vivo imaging technology now allow one to characterize the responses of different types of inhibitory neurons in the mouse V1 in awake animals that are free to run (Dombeck et al., 2010; Harvey et al., 2012; Taniguchi et al., 2011).

By crossing Ai14 (Cre-dependent TdTomato reporter) mice with vasoactive intestinal peptide (VIP)-Cre mice (Madisen et al., 2010; Taniguchi et al., 2011), we labeled VIP-positive GABAergic neurons genetically. We then imaged the calcium responses of these VIP neurons in freely running head-fixed mice with or without visual stimulation. We found that the neural activity of VIP neurons in mouse V1 is closely correlated with the locomotion even without visual stimulation, when most other neurons in the visual cortex show only spontaneous activity. Visual stimulation, which drove the other cortical neurons, did not increase the activation of VIP neurons by locomotion. A similar approach revealed that somatostatin (SST) neurons were inhibited by locomotion, consistent with a circuit in which VIP cells increase activity of neighboring excitatory cells by inhibiting their inhibitory input from SST cells (Pfeffer et al., 2013). Also consistent with this circuit, parvalbumin (PV) neurons showed heterogeneous responses to locomotion. The local blockade of nicotinic cholinergic input, but not of glutamatergic input, reduced the response of VIP neurons to locomotion by more than two thirds, and

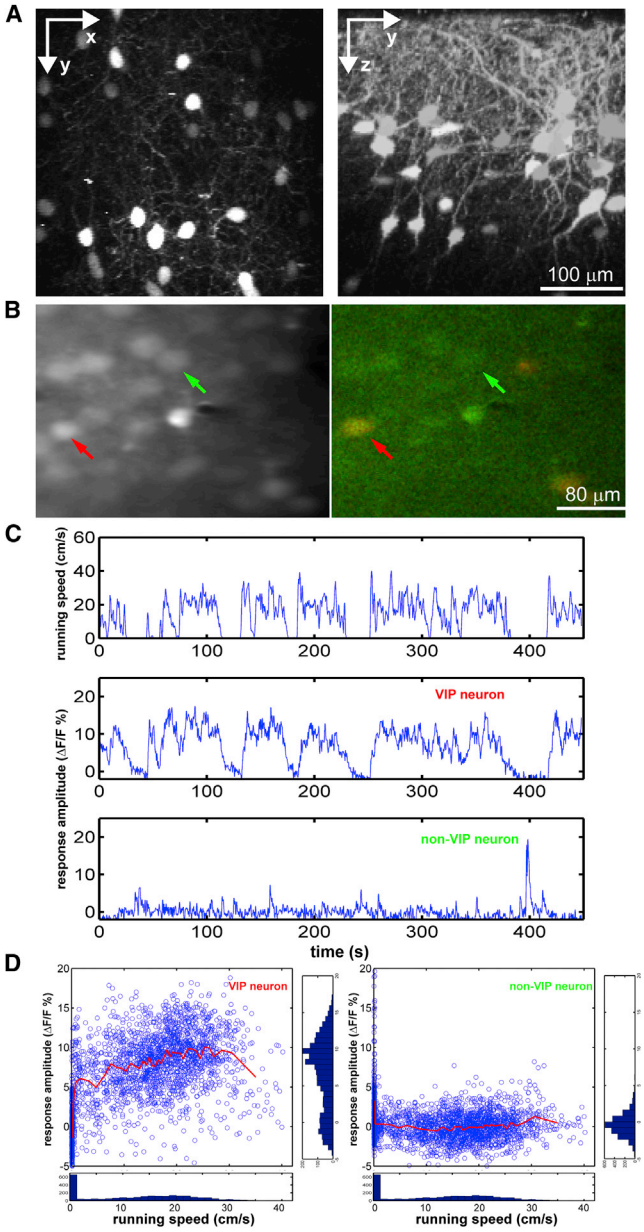

Figure 1. Calcium Imaging of VIP Neurons In Vivo in Behaving Mouse

(A) Images in vivo of V1 in VIP-Cre::Ai14 mouse. Left: projection along z-axis, and is a "top-down view" of the brain showing the lateral distribution of VIP neurons. Right: projection along x axis, and is a "side view" of the brain showing the distribution of VIP neurons across different cortical layers.

(B) After loading OGB-1, images were taken at 800 nm (green channel only, left) to image the calcium response, and at 910 nm to visualize the TdTomato-expressing VIP neurons (right). Red arrows point to a VIP neuron; green arrows indicate a non-VIP neuron.

(C) Example showing calcium responses of the VIP (middle) and non-VIP (bottom) neurons shown in (B) in relation to running speed (top).

(D) The distribution of the calcium signal in relation to the running speed for each signal point of the traces in (C). The side panels show the count of signal points along corresponding axis. The red line is the average fluorescent value along the running axis smoothed with a 50-data point sliding window.

measurements in vitro disclosed powerful nicotinic cholinergic input to VIP neurons. Rabies-virus-based retrograde tracing (Wickersham et al., 2007) showed that the upper layer VIP neurons in V1 receive direct input from the nucleus of the diagonal band of Broca (NDB), a cholinergic center in basal forebrain. Finally, activating VIP neurons in mouse V1 optogenetically in stationary mice mimicked the effect of locomotion and increased the visual responses of neurons in V1, while focal damage to VIP neurons blocked the enhancement of cortical responses by locomotion. Interestingly, VIP neurons in other sensory cortices also responded to locomotion, though less vigorously than in V1. Our findings therefore reveal a cell-type-specific circuit that mediates the enhancement of visual response by locomotion. We suggest that this circuit may be a common pathway mediating behavioral state-dependent gain control in the neocortex.

RESULTS

VIP Neurons in V1 Respond to Locomotion

We first examined whether we could observe the increase of visual response induced by running using in vivo calcium imaging. Using an apparatus that allows the mouse to run freely on a styrofoam ball floating on air while its head is fixed in space (Dombeck et al., 2010), we recorded the trackball movement and calcium signals simultaneously using two-photon imaging of neurons loaded with Oregon Green BAPTA (OGB-1), allowing us to analyze the calcium response of many single neurons in relation to locomotion (Figures S1A and S1D available online). We then calculated a "locomotion modulation index" by dividing the calcium response amplitude during locomotion by its amplitude in the stationary state separately for each orientation of visual stimulus gratings (Figures S1C and S1F). On average, running led to an increase of 37% ± 7% in the calcium response (Figure S1G), demonstrating that our in vivo calcium imaging system is able to reproduce the findings made electrophysiologically (Niell and Stryker, 2010).

To study VIP neurons, we genetically labeled VIP-positive GABAergic neurons by crossing VIP-Cre mice with Ai14, a cre-dependent TdTomato reporter line. VIP neurons are present in both upper and deep layers, as shown previously (Taniguchi et al., 2011). In vivo two-photon imaging in V1 of VIP-Cre::Ai14 mice allowed us to visualize the dendrites and cell bodies of VIP neurons in upper layers (layer I to II-III) (Figure 1A). We then imaged the calcium responses of VIP neurons 150–300 μm below the pia, using two-photon microscopy during locomotion and stationary alertness. After OGB-1 loading, the VIP neurons could be readily identified under 910 nm excitation (Figure 1B, red arrow), while the calcium imaging was performed under 800 nm (Figure 1B).

We first examined whether the activity of VIP neurons is correlated with locomotion in the absence of visual stimulation in darkness. To our surprise, while non-VIP neurons (Figure 1B, green arrow) showed only low-frequency spontaneous calcium spikes similar to those when the animal was stationary, the calcium responses of VIP neurons were greatly elevated during locomotion (Figure 1C). The change from the stationary (running speed < 1 cm/s) to the "running" state (running speed > 1 cm/s) was evident when the calcium traces were plotted with the

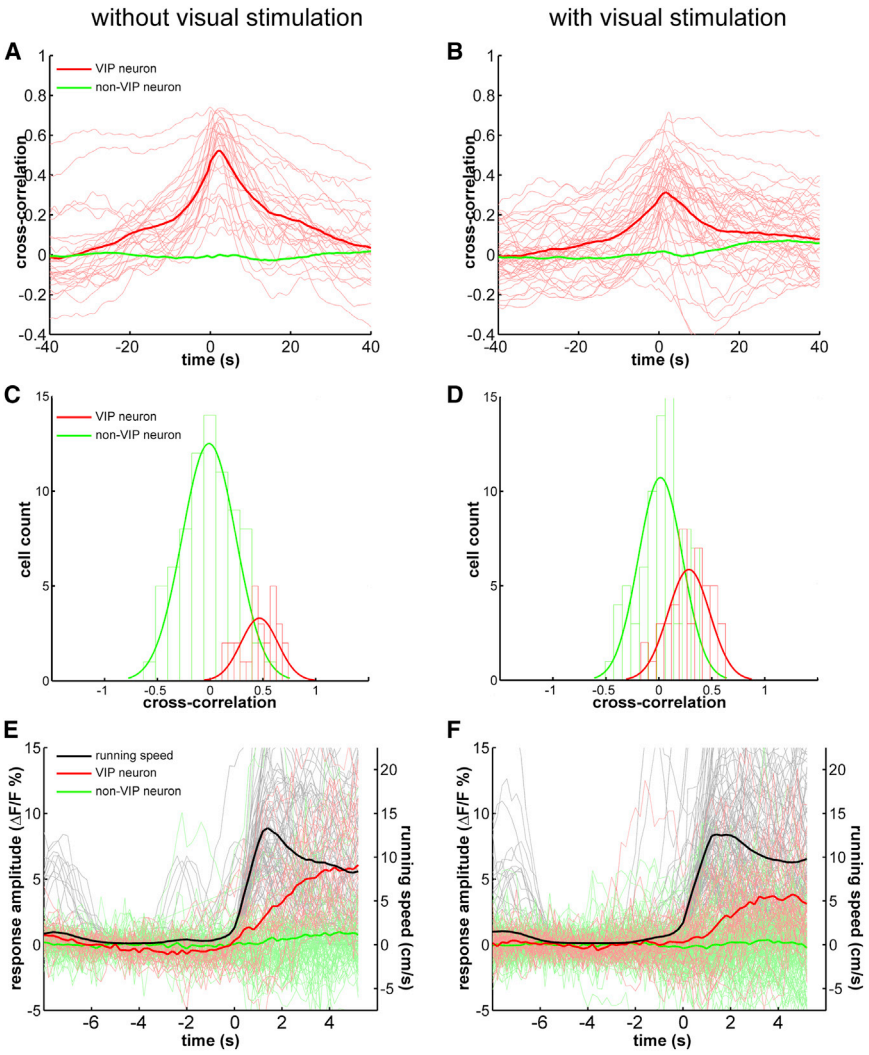

Figure 2. Calcium Responses of VIP Neurons Are Closely Correlated with Running and Are Modulated by Visual Stimulation

(A and B) The cross-correlation between the calcium response and running speed chart, when imaged with (A) or without (B) visual stimulation. The thin red lines are the cross-correlation curves of all recorded VIP neurons (A, n = 28, 4 mice; B, n = 44, 7 mice). The thick red curve is the average of all thin red curves. The thick green curve is the average of the cross-correlation curves of all recorded non-VIP neurons (A, n = 77, 4 mice; B, n = 76, 7 mice).

(C and D) The distribution of the zero-time cross-correlation value of all recorded VIP and non-VIP neurons, when imaged with (C) or without (D) visual stimulation. The green and red curves are fitted curve with Gaussian distribution.

(E and F) The calcium responses of VIP (red traces) and non-VIP neurons (green traces) aligned to the running episodes (black traces), when imaged with (E) or without (F) visual stimulation. Each thin trace (red or green) is the average of all extracted responses of a single cell.

running speed (Figure 1D). In contrast, the calcium responses of nearby non-VIP neurons were not increased during locomotion (Figure 1D, red lines). Like the visual responses of excitatory neurons in V1 (Figure 3G of Niell and Stryker, 2010), the calcium responses of the VIP neurons in the running state were only weakly (though significantly) modulated by changes in running speed. The effects of locomotion on the responses of the VIP neurons in the absence of visual stimulation were therefore distinct from those of nearly all non-VIP neurons.

Analysis of all VIP neurons imaged under conditions of no visual stimulation by calculating the cross-correlation between the calcium signal and running speed revealed a single positive peak around time zero (0.47 ± 0.03, mean ± SEM, n = 28) (Figure 2A). The activities of non-VIP neurons were in general not altered by locomotion in the absence of visual stimulation. While 20/28 imaged VIP neurons had a zero-time cross-correlation larger than 0.4, only 3/77 non-VIP neurons had a zero-time cross-correlation larger than 0.4 (Figure 2C), indicating that VIP neurons constitute the majority of the neurons responsive to locomotion in the absence of visual stimulation in mouse V1.

Visual Stimulation Does Not Increase the Response of VIP Neurons in V1 to Locomotion

A signal conveying behavioral state to sensory cortex would ideally not be confounded by the sensory response that it modulates. Interestingly, we found that the cross-correlation between the VIP neurons' calcium responses and locomotion was not increased by visual stimulation with drifting gratings, and indeed was significantly reduced (0.28 ± 0.03, mean ± SEM, n = 44, $p < 0.0001$ comparing with no visual stimulation group, Mann-Whitney U test) (Figure 2B and Figure S2A for paired comparison of the 12 neurons imaged under both conditions). The distribution of all VIP neurons' cross-correlations shifted toward lower value, while the distribution of non-VIP neurons, the responses of which were time locked to the visual stimuli rather than to locomotion, did not change (Figure 2D). Although the responses of the majority of neurons were positively modulated by locomotion, the average cross-correlation between locomotion and the calcium responses of non-VIP neurons did not show a positive peak, because the episodes of running were independent of the onset of visual stimulation.

To further analyze the response of VIP neurons to locomotion, we extracted all running "episodes" for which the mouse was stationary (average speed < 1 cm/s) during the 5 preceding seconds and aligned the calcium response to the start of running. While each mouse had varying numbers of such running episodes, we averaged all such aligned events for each neuron and to produce an averaged trace for each neuron (Figure 2E, each faint red trace is one VIP neuron). We then averaged the response traces of all neurons and found the averaged response

of VIP neurons to running was 5.42% ± 0.66% of baseline level (Figure 2E, dark red trace). Such alignment further illustrates the tight coupling between VIP calcium response and running. The same analysis was also done for neurons imaged during visual stimulation, and we found that the response amplitude of VIP neurons was 3.53% ± 0.56% (mean ± SEM) of baseline level ($p = 0.017$ comparing with no visual stimulation group, Mann-Whitney U test), while the average running speed was similar (Figure 2F and Figure S2B for paired comparison of the 12 neurons imaged under both conditions). Such decrease of VIP neurons' response to locomotion under visual stimulation may result from increased inhibitory drive from visually activated inhibitory neurons. The reduced locomotion response and VIP neurons' response to visual stimulation (Figures S2C and S2D) may both contribute to the decreased cross-correlation. Nevertheless, VIP neurons responded strongly and faithfully to locomotion both during and in the absence of visual stimulation.

Locomotion Differentially Modulates Responses of Other Inhibitory Neurons

To determine how selectively locomotion activates VIP and other inhibitory neurons, we examined the calcium responses of PV and SST neurons under the same conditions as those used for VIP neurons. We first examined the responses of three major inhibitory neuron classes using adeno-associated viral (AAV) transfection of floxed GCaMP6s into the specific Cre-expressing mice (Chen et al., 2013). For VIP neurons, the calcium signal from GCaMP6 was again closely associated with locomotion. The cross-correlation between the GCaMP6 signal and locomotion is consistent with the results in Figure 2A, and the distribution of the zero-time cross-correlation showed a single peak with a value near 0.5 (Figure 3A). The responses of PV neurons were heterogeneous. Many PV neurons were positively associated with locomotion, while others were suppressed by locomotion (Figures S3A and S3B). The cross-correlation curves were also heterogeneous, making the distribution of zero-time cross-correlations bimodal, with one group peaking around 0.5 and the other peaking at a negative value (Figure 3B). On the other hand, the calcium responses of SST cells were suppressed by locomotion (Figure S3C). The average cross-correlation of SST neuron activity with locomotion was negative at time-zero, and the distribution of zero-time cross-correlation had a single negative peak (Figure 3C). Furthermore, the average calcium signal of SST neurons was consistently reduced by running (Figure S3D, left, normalized signal during running versus stationary, $p < 0.001$, paired t test). On average, the zero-time cross-correlation of VIP neurons was 0.58 ± 0.03 ($n = 21$), significantly different from that of PV neurons (0.30 ± 0.06, $n = 40$, $p = 0.01$, rank-sum test), and SST neurons was −0.19 ± 0.05 ($n = 11$, $p < 0.005$ comparing with 0, t test), which were also different from each other (Figure 3D, $p < 0.0001$, one-way ANOVA). Similar results were also obtained using OGB-1 in TdTomato labeled PV or SST neurons (Figure S3D, right, normalized signal during running versus stationary, $p < 0.001$; and Figures S3E–S3G).

By aligning calcium responses to the start of running events, the GCaMP6 signal of VIP neurons on average increased 155.0% ± 34.8%, and the distribution of cross-correlations of the extracted events and calcium signal had a single peak at 0.7 (Figure 3E). The majority of the PV neurons responded to the start of running, but many responses were small or negative (Figure 3F), resulting in a lower average response amplitude (105.0% ± 23.2%) comparing to that of VIP neurons (Figure 3H). For SST neurons, no significant GCaMP6 signal was precisely aligned to the start of running (Figure 3G). Similar results were also found using OGB-1 in TdTomato labeled PV and SST neurons (Figures S3H–S3J).

Qualitatively, the responses of VIP neurons differed from those of PV and SST neurons by remaining elevated throughout the period of locomotion in the dark; while those PV neurons whose activity increased with the onset of locomotion were less tightly coupled, many falling nearly to baseline before the animal became stationary. By aligning GCaMP6 signal to the end of running events, all VIP neurons showed a clear reduction of calcium signal in response to the decreasing running speed, and all but one extracted event were strongly positively correlated with time at which locomotion ceased (Figure 3I). On average, the calcium signal of VIP neurons reduced from 91.1% ± 13.8% higher than baseline to baseline when the animal transited from running to stationary (Figure 3L). While a few PV neurons responded like VIP neurons, many did not show a clear response to the end of running, and the distribution of the cross-correlation of extracted events was distributed broadly around 0 (Figure 3J). The average calcium signal of PV neurons declined from 34.0% ± 6.5% higher than baseline to baseline when the animal transitioned from running to stationary (Figure 3L), about 1/3 of that of VIP neurons. On the other hand, the ending of running events resulted in an increase of the calcium signal of SST neurons, because some neurons started firing immediately after end of running (Figure 3K), and the calcium signal of SST neurons just before the end of running was near baseline (5.1% ± 11.9%) (Figure 3L).

Nicotinic Activation of VIP Neurons by Locomotion

Stimulation of basal forebrain has been reported to activate VIP neurons in V1 through nicotinic acetylcholine receptors (nAChRs) (Alitto and Dan, 2012). The midbrain locomotor center including the pedunculopontine tegmental nucleus (PPTg) projects to multiple subcortical and cortical areas, as well as to basal forebrain (Garcia-Rill, 1991; Newman et al., 2012). We sought to identify the afferent pathways mediating activation of upper-layer VIP neurons during locomotion by imaging VIP neurons' response after local infusion of different channel blockers into V1 (Figure 4A). After loading OGB-1, an Alexa-594 loaded pipette with either control loading buffer solution or drug solution was placed close to the OGB-1-loaded area (Figure 4B). We first injected 500 nl of loading buffer, and found no effect on the response of VIP neurons to locomotion in the absence of visual stimulation (zero-time cross correlation: loading buffer injection 0.46 ± 0.05, $n = 11$, no injection 0.47 ± 0.03, $n = 28$; response amplitude: loading buffer injection 5.92% ± 0.77%, no injection 5.42% ± 0.66%) (Figures 4C and 4D, red traces comparing with Figures 2A and 2E). Local injection of the glutamate receptor antagonist NBQX (1 mM) also did not change the response to locomotion (zero-time cross correlation: 0.36 ± 0.09; response amplitude: 6.62% ± 2.58%, $n = 9$) (Figures 4C and 4D, blue traces). In contrast, a similar injection of the nAChRs antagonists

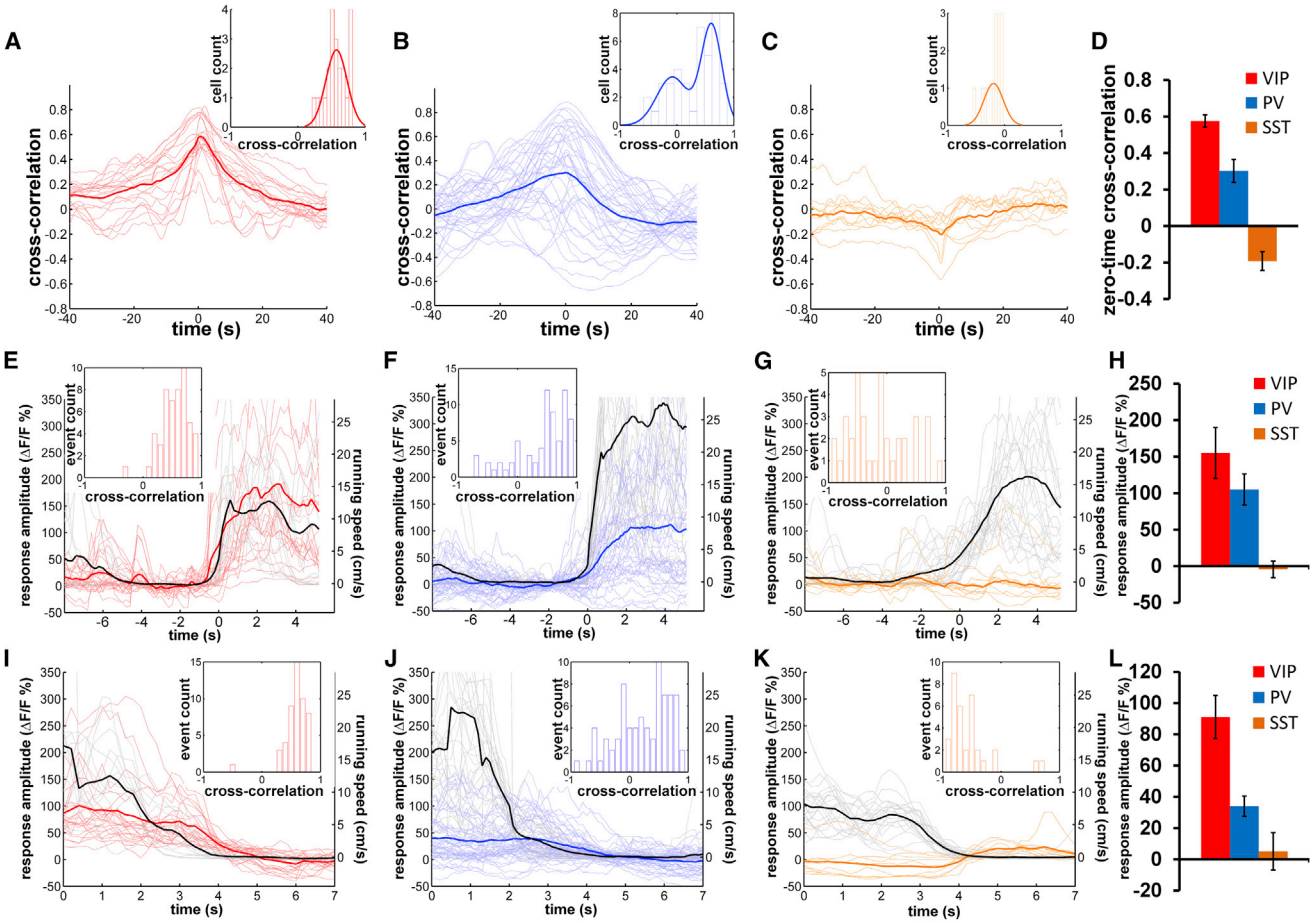

Figure 3. Locomotion Differentially Modulates the Responses of Different Types of Inhibitory Neurons

(A–C) The cross-correlation between the GCaMP6s calcium signal and running speed chart for VIP (A), PV (B), and SST (C) neurons. The thin lines are the cross-correlation curves of all recorded neurons (A, n = 21; B, n = 40; C, n = 11). The thick curve is the average of all thin curves. Insert histograms show distribution of zero-time cross-correlation values, and the curves are fitted with single or double-Gaussian functions.

(D) The average zero-time cross-correlation for three different inhibitory neurons (mean ± SEM).

(E–G) The calcium responses of VIP (E), PV (F), and SST (G) neurons are aligned to the start of running episodes (black traces). Each thin trace is the average of all extracted events of a single neuron, and the thick trace is the average of all thin traces. Insert histograms show distribution of zero-time cross-correlation values between extracted running speed and calcium signal change of all extracted events of all neurons.

(H) The average calcium response amplitude of the three types of inhibitory neurons. The values plotted are the average of the curves between 2 s and 4 s on the x axis in (E–G) (mean ± SEM).

(I–K) The calcium responses of VIP (I), PV (J), and SST (K) neurons are aligned to the end of running episodes (black traces). Each thin trace is the average of all extracted events of a single neuron, and the thick trace is the average of all thin traces. Insert histograms show distribution of zero-time cross-correlation values between extracted running speed and calcium signal change of all extracted events of all neurons.

(L) The average calcium response amplitude of three types of inhibitory neurons. The values plotted are the average of the curves between 1 s to 3 s on the x axis in (I–K) (mean ± SEM).

mecamylamine (MEC) and methylycaconitine (MLA) (1 and 0.1 mM, respectively) did not block the visual responses of nearby non-VIP neurons (Figures S4A–S4F), but dramatically reduced the responses of VIP neurons to locomotion (zero-time cross correlation: 0.16 ± 0.05; response amplitude: 1.5% ± 0.46%, n = 27) (Figures 4C and 4D), without, of course, changing the locomotion speed (Figure 4E). Furthermore, local injection of NBQX blocked the effect of visual stimulation on VIP neurons' response to running (Figures S4G and S4H, comparing with Figures S2A and S2B), indicating the effectiveness of NBQX in the blockade of visually driven neuronal activation. It should be noted, however, that the response of VIP neurons to locomotion in the absence of visual stimulation was not completely abolished by nAChRs antagonists, indicating that there are probably other sources of locomotory input to VIP neurons.

These findings in vivo suggest that acetylcholine (ACh) activates VIP neurons directly through nAChR. In acute cortical slices, local puffing of ACh (100 μM) reliably elicited action potentials in VIP neurons in V1 (Figure S5A). In the presence of

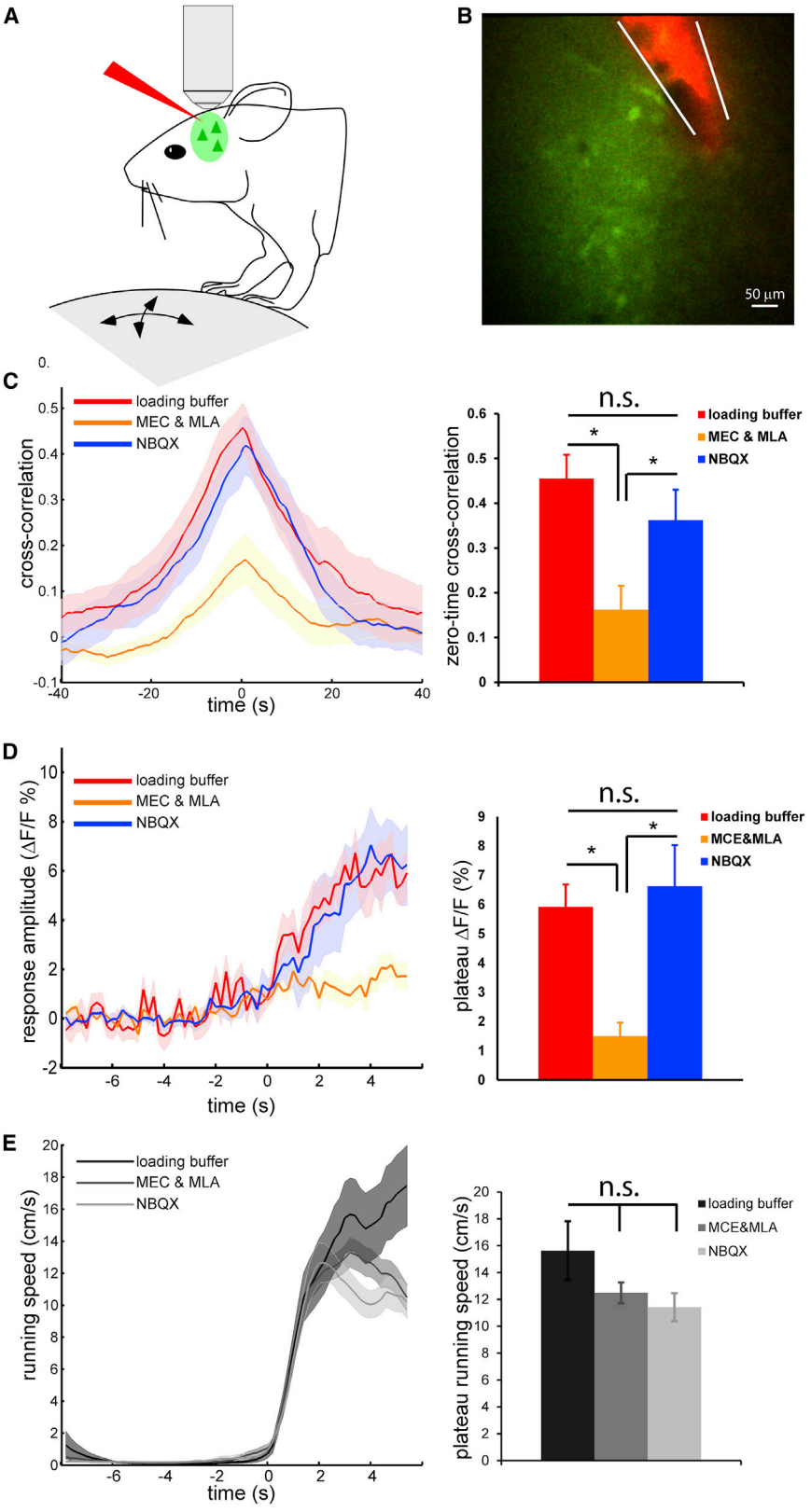

Figure 4. Activation of VIP Neurons by Locomotion via nAChRs

(A) Diagram showing the experimental setup. Mouse with fixed head is free to run on a Styrofoam ball floating on air. After loading OGB-1, a glass pipet loaded with Alexa-594 and drug solutions is placed near the OGB-1 loading area under two-photon imaging.

(B) An example showing drug pipette and OGB-1 loading.

(C) Left: cross-correlation between calcium response and running speed of VIP neurons during local infusion of different drug solutions (mean ± SEM; loading buffer, n = 11, 3 mice; MEC&MLA, n = 27, 4 mice; NBQX, n = 17, 3 mice), when imaged without visual stimulation. Right: zero-time cross-correlation values of VIP neurons under different drug conditions (mean ± SEM, *p < 0.01, one-way ANOVA and Bonferroni post hoc test).

(D) Left: calcium response aligned to each running episodes (mean ± SEM). Right: plateau response amplitude of calcium responses aligned to running (mean ± SEM).

(E) No effect of drug infusion on locomotion. Left: extracted running episodes under different drug conditions (mean ± SEM; loading buffer, n = 23; MEC&MLA, n = 89; NBQX, n = 37). Right: running speed corresponding to the plateau calcium response shown in (D) (mean ± SEM, *p > 0.05, one-way ANOVA and Bonferroni post hoc test).

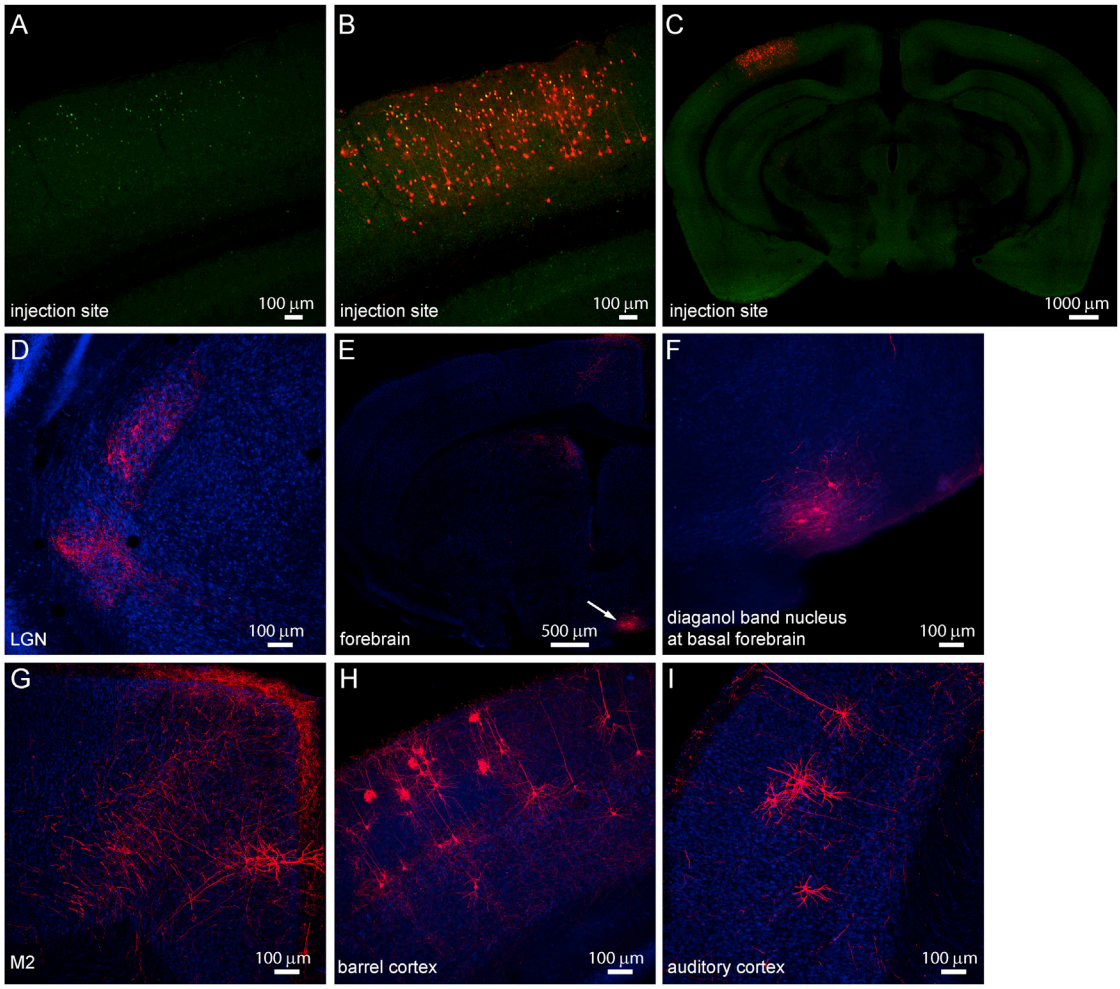

Figure 5. Retrograde Labeling of Monosynaptic Inputs to Upper Layer VIP Neurons in Mouse V1

(A) AAV2/9-TRE-HTG was injected into V1 of VIP-Cre: ROSA-LSL-tTA mouse, and rabies virus (EnvA-SAD-ΔG-mcherry) was injected 2 weeks later into the same site. VIP neurons expressing hGFP were restricted to the upper layer.

(B) The local input neurons to hGFP-expressing VIP neurons express mCherry and are located across different layers of V1.

(C) Zoom-out view of the brain slice showing the injection site in V1.

(D) Sparse labeling of input neurons and neurites in and near LGN.

(E) Coronal section of the forebrain showing labeling of basal forebrain nucleus.

(F) Zoom-in view of the labeling of diagonal band nucleus.

(G) mCherry-expressing neurites and a pyramidal neuron in M2.

(H) Labeling of pyramidal neurons in barrel cortex.

(I) Labeling of pyramidal neurons in auditory cortex.

tetrodotoxin (TTX), the depolarization induced by ACh was abolished by the nAChR blockers MEC&MLA (12.41 ± 0.98 mV versus 2.61 ± 0.26 mV, $p < 0.01$, Figures S5B and S5C), confirming the existence of direct nicotinic cholinergic responses in VIP neurons.

To further investigate the input to upper layer VIP neurons in V1, we used rabies virus to trace their monosynaptic inputs (Wickersham et al., 2007). By restricting the depth of the virus injection pipette, we tried to target the upper layer VIP neurons in V1 (Figures 5A–5C). As expected, many V1 neurons were labeled as direct input neurons, and sparse neurons in LGN were also labeled (Figure 5D). Interestingly, such retrograde tracing identified the nucleus of the diagonal band of Broca (NDB), a basal forebrain nucleus enriched of cholinergic neurons, as a prominent source of input to upper layer VIP neurons in V1 (Figure 5E white arrow, 5F, and S6).While we labeled more than 50 upper layer VIP neurons in V1, only 0–1 neuron per mouse was retrogradely labeled in motor cortex or the border between motor and cingulate cortex (Figure 5G), suggesting at most very sparse direct input from motor cortex. Surprisingly, a considerable number of pyramidal neurons in multiple layers of primary somatosensory barrel cortex, and some neurons in primary auditory cortex showed retrograde labeling (Figures 5H and 5I).

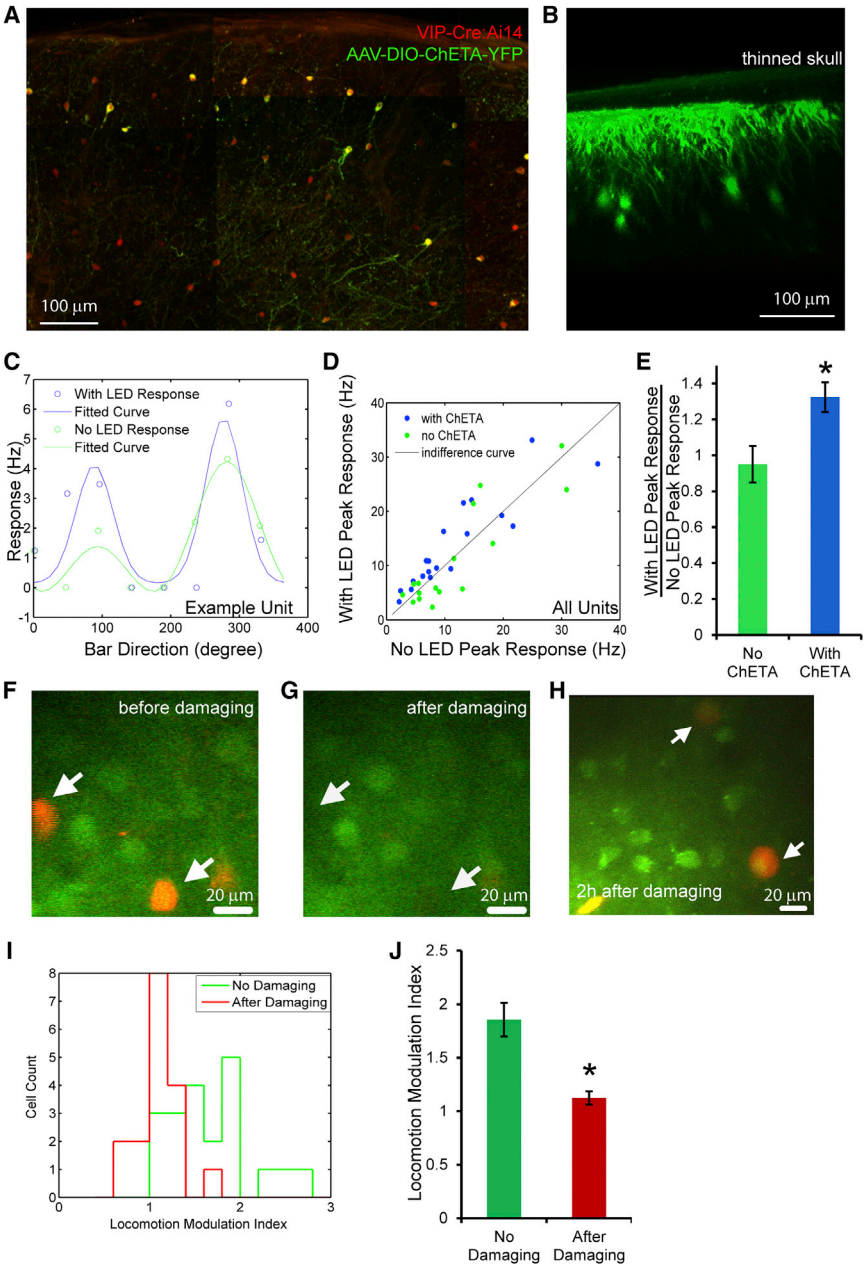

Figure 6. VIP Neurons Sufficient and Necessary for Modulation of Gain of Visual Responses by Locomotion

(A) Section of the visual cortex of a VIP-Cre:Ai14 mouse injected with AAV-DIO-ChETA-YFP. All VIP-Cre cells express tDTomato (red) and infected neurons also express ChETA-YFP (green).

(B) Imaging in vivo of VIP neurons infected with AAV-DIO-ChETA-YFP through thinned skull craniotomy.

(C) Orientation tuning of an isolated unit in control (No LED, green) condition and during optogenetic activation of VIP neuron (With LED, blue) condition, in a stationary VIP-Cre:Ai14 mouse injected with AAV-DIO-ChETA-YFP. Response values are average of five trials using moving bars; orientation tuning curves are fitted with double-Gaussian function.

(D) Comparison of peak responses of isolated units in stationarymouse during control (No LED) condition and during optogenetic activation of VIP neuron (With LED) condition, in VIP-Cre:Ai14 mouse injected with AAV-DIO-ChETA-YFP (blue circles, 19 units, 3 animals) or without AAV injection (green circles, 16 units, 2 animals).

(E) Average values of the ratio between With LED peak response and No LED peak response, of all the isolated units in either AAV-DIO-ChETA-YFP injected (blue bar) or no AAV injected (green bar) VIP-Cre:Ai14 animals (mean ± SEM, *p < 0.009 comparing with "No ChETA" group, Mann-Whitney U test).

(F–J) Photolytically damaging VIP neurons abolishes increase of visual response induced by locomotion in non-VIP neurons. After loading OGB-1 into the V1 of VIP-Cre::Ai14 mice, area of interest was imaged before (F) and after (G) photolytic damaging of VIP neurons. Arrows indicate two VIP neurons. (H) VIP neurons become round and swollen 2h after photolytic damage. Arrows indicate two such VIP neurons. (I) The distribution of the locomotion-modulation-index (visual response during locomotion / visual response when stationary), of the "No Damaging" (n = 22) and "After Damaging" (n = 17) groups. (J) Average values of locomotion-modulation-index for "No Damaging" and "After Damaging" groups. (mean ± SEM, *p < 0.0001 comparing with "No Damaging" group, rank-sum test).

VIP Neurons Are Key Mediators of the Enhancement of Visual Responses by Locomotion

It has been reported that VIP neurons in V1 strongly inhibit SST-positive inhibitory neurons (Pfeffer et al., 2013), whose activation results in suppression of the visual response of excitatory neurons (Adesnik et al., 2012). Our data and the previous reports (Niell and Stryker, 2010) therefore provide a plausible mechanism by which VIP neurons could contribute to the increase of visual response induced by running. To test directly the involvement of VIP neurons in increasing the visual responses of excitatory neurons, we conditionally expressed channelrhodopsin in upper layer VIP neurons in V1 using viral injection of a flexed ChETA vector into VIP-Cre:Ai14 mice (Figure 6A). Through the thinned skull for in vivo recording, we could readily image the dendrites and cell bodies of ChETA-expressing VIP neurons in V1 (Figure 6B). To determine the impact of activating VIP neurons on the visual response of V1 neurons, we performed extracellular recordings as described in Supplemental Information and alternated trials in which VIP neurons were optogenetically-activated (using a blue light, referred to as LED condition) with control trials (No LED condition) (Figure 6C). Photo-activation of VIP neurons in awake stationary mice significantly increased the visual response of layer 2/3 neurons by 32.4% ± 8.3% (mean ± SEM; n = 19, p < 0.02, paired Wilcoxon signed rank test) without producing locomotion or changing the orientation selectivity index (OSI) (Figure S7A), while a similar procedure of LED illumination

did not produce significant effects in the animals without ChETA virus injection (peak response change: −5% ± 10.2%, mean ± SEM; n = 16, p = 0.47, paired Wilcoxon signed rank test) (Figure 6D). The increase in visual response induced by VIP optogenetic activation was highly significant ($p < 0.009$, Mann-Whitney U test, comparing LED activation in ChETA versus control animals without virus injection) (Figure 6E). Therefore, activating VIP neurons in stationary animals is sufficient to produce an increase in the visual response similar to that induced by running.

To investigate the necessity of VIP activation in the increase of visual response induced by running, we photolytically damaged VIP neurons and examined the visual responses of nearby non-VIP neurons. By restricting the scan area briefly to a single-cell diameter and repeating this procedure one by one over the upper layer VIP neurons in the microscope field, we used the excitation beam to photolytically damage the VIP neurons in a small region of cortex without bleaching the OGB-1 signal of nearby non-VIP neurons (Figures 6F and 6G). VIP neurons damaged in this way were first bleached of TdTomato signal but revealed themselves as swollen after 1–2 hr (Figure 6H). While the nearby non-VIP neurons still responded to visual stimulation, the enhancement of their activity by locomotion was significantly reduced (86% ± 16% enhancement without photo damage versus 12% ± 6% enhancement after photo damage; $p < 0.0001$, rank-sum test) (Figures 6I and 6J). Taken together, these findings indicate that VIP neuron activation is both necessary and sufficient for the increase in the visual response of excitatory cells produced by locomotion.

VIP Neurons in other Primary Sensory Cortices also Respond to Locomotion

Considering the similar distribution pattern of VIP neurons through the cortical areas, and the broad projection of NDB to other cortical areas, we examined whether VIP neurons in other primary sensory cortices are also modulated by locomotion. We first looked at the primary somatosensory barrel cortex and found the response of VIP neurons tightly locked to the locomotor activity (Figure 7A). When aligning the fluorescent traces to the running events, the averaged traces of all VIP neurons showed a clear correlation with the averaged running trace (Figure 7B). However, although the mice were running in darkness with no visual input, the whiskers were intact and the mice were free to move them. Although the cross-correlations were in general much lower than that in visual cortex (Figure 7C), the averaged cross-correlation between calcium responses and locomotion in VIP neurons was significantly different from that in non-VIP neurons (0.15 ± 0.08 versus −0.05 ± 0.04, p = 0.047, Mann-Whitney U test, Figure 7D), Furthermore, the locomotion response of VIP neurons was also significantly higher than that of non-VIP neurons (2.75% ± 0.98% versus 0.13% ± 0.66%, p = 0.022, Mann-Whitney U test, Figure 7D).

The responses of VIP neurons in primary auditory cortex were also associated with locomotor activity (Figure 7E), though much less strongly so than those of V1. The aligned fluorescent traces of all VIP neurons deviated significantly, although only slightly, from those of non-VIP neurons (Figure 7F). Our setup was far from ideal in isolating auditory inputs, which might result in a lower level of cross-correlation (Figure 7G). However, the zero-time cross-correlation of VIP neurons was still significantly higher than those of non-VIP neurons (0.22 ± 0.08 versus −0.02 ± 0.06, p = 0.043, Mann-Whitney U test, Figure 7H). Likewise, the locomotion response of VIP neurons was significantly greater than that of non-VIP neurons (3.00% ± 1.31% versus −0.33% ± 0.31%, p = 0.022, Mann-Whitney U test, Figure 7H).

DISCUSSION

Sensory responses have long been known to be modulated by behavioral state, but the neural circuit responsible for this modulation has remained obscure (Maunsell and Cook, 2002; Niell and Stryker, 2010; Reynolds and Chelazzi, 2004; Wurtz and Mohler, 1976). Locomotion in the mouse is an easily measured, tractable behavioral state that profoundly increases specific visual responses in V1 without changing selectivity (Niell and Stryker, 2010). This modulation of V1 activity is thought to arise in the cortex because locomotion produces no parallel increase in the responses of neurons in the LGN that provide the visual input to V1 (Niell and Stryker, 2010).

The present study reveals that a specific type of GABAergic cortical neuron, the VIP neuron, transmits the signal of locomotion to the cortex and operates through disinhibition of another GABAergic cortical neuron, the SST cell, to enhance the responses of neighboring cortical excitatory neurons (Pfeffer et al., 2013). Evidence for this conclusion includes the consistent activation of VIP cells by locomotion in darkness (when neighboring excitatory neurons are silent) or in light; the fact that VIP cell responses vary as a function of walking speed in a way that mirrors the enhancement of excitatory cell visual responses; the facts that optogenetic activation of VIP cells mimics the effect of locomotion in stationary mice and that damage to VIP cells blocks the enhancement of excitatory cell visual responses by locomotion; the monosynaptic input to VIP cells from a cholinergic nucleus in the basal forebrain together with the direct nicotinic cholinergic activation of VIP cells in vitro and the substantial reduction of their responses to locomotion by nicotinic blockers in vivo; and the consistent inhibition of SST cells in alert animals in vivo by locomotion. These findings establish the VIP cells as a critical element of the cortical circuit that is responsible for the effects of locomotion on visual responses in mouse V1. The presence of elements of this circuit throughout the cortex suggests that VIP cell activation may be a general mechanism for cortical gain control by behavioral state.

Sensory-motor integration in rodents has been studied extensively in primary somatosensory barrel cortex, in which whisker movement and sensory information are sent to different segments of the same pyramidal neuron (Crochet et al., 2011; Petreanu et al., 2012; Xu et al., 2012). In barrel cortex the SST neurons become hyperpolarized and fire fewer action potentials during active or passive whisker stimulation, in contrast to neighboring neurons that are excited by stimulation (Gentet et al., 2012). This finding is consistent with the possibility that a circuit similar to that in V1 may operate in barrel cortex. Interestingly, it is recently reported that VIP neurons in barrel cortex are strongly activated by vibrissal motor cortex pyramidal neurons (Lee et al., 2013).

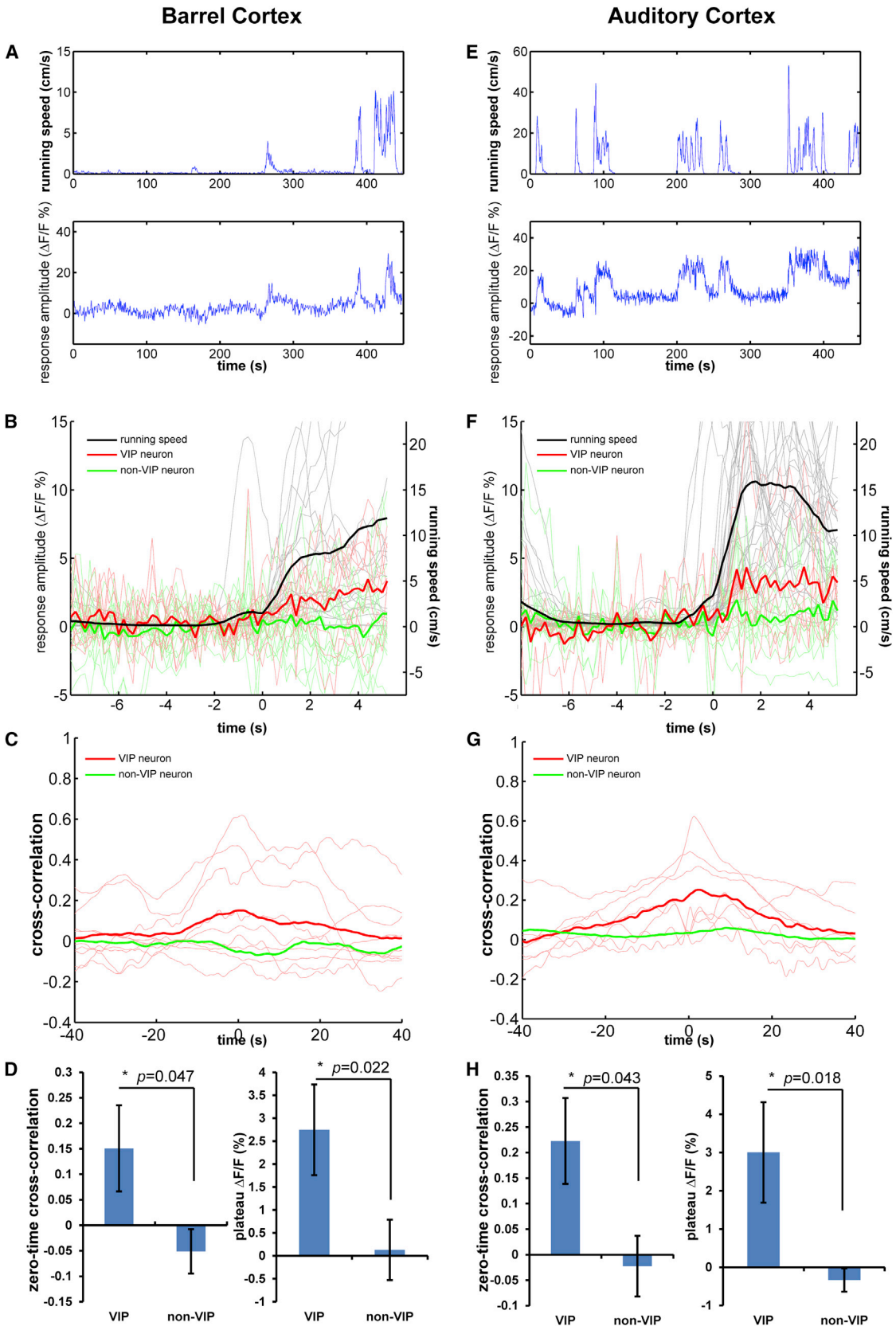

(legend on next page)

Our finding that locomotion activates VIP neurons largely through cholinergic input is consistent with a role for acetylcholine in modulating the visual response. Acetylcholine has been demonstrated to play important roles in cortical activation and attentional modulation in many systems (Hasselmo and Giocomo, 2006; Weinberger, 2007). Cholinergic input has been shown to modulate several aspects of visual response, such as the shift of local-field-potential spectrum and response magnitude (Metherate et al., 1992; Rodriguez et al., 2004; Sato et al., 1987a; Sato et al., 1987b), similar to what we have observed for locomotion (Niell and Stryker, 2010). Stimulation of the basal forebrain has been shown to activate VIP neurons and layer I interneurons through nAChRs, though not necessarily directly (Alitto and Dan, 2012; Arroyo et al., 2012). Although we found that VIP neurons receive input from NDB, they may also receive inputs from other neuromodulatory sources, which might not be revealed due to the low efficiency of the rabies-virus-mediated retrograde tracing. The fact that we were not able completely to block the response of VIP neurons to locomotion using nicotinic antagonists makes a role for other neuromodulatory inputs seem likely. For example, a recent study suggested a role of noradrenergic input (Polack et al., 2013).

It should also be kept in mind that the basal forebrain responds to many different stimuli and may influence cortical response by modulating different populations of neurons. For example, the neurons in NDB and nearby nuclei have been found to respond not only to locomotion but also to other stimuli such as females (in male mice) and water (Mink et al., 1983). Furthermore, different inhibitory neurons may be modulated by cholinergic inputs in different manners (Arroyo et al., 2012; Kawaguchi, 1997). Although it was previously shown that 5-HT3a receptor-positive neurons, among which VIP neurons are a major population, are depolarized by nicotine and show no response to muscarine (Lee et al., 2010), there was no direct evidence that ACh activates VIP neurons through nAChR. The present study shows that ACh depolarizes VIP neurons strongly enough to elicit action potentials through nicotinic receptors. No fast nAChR component like that shown in layer I inhibitory neurons (Letzkus et al., 2011) was evident; our findings showed instead a response with slow kinetics resembling what has been found in ChAT-positive bipolar neurons (Arroyo et al., 2012). Therefore, it is likely that VIP neurons are activated by ACh through non-α7 nAChR.

It was initially surprising that inhibitory VIP neurons were directly activated by locomotion in the dark when we knew that locomotion increased visual responses. Recent advances in mouse genetics, allowing targeted recordings of different types of GABAergic interneurons, have revealed some of the relevant circuitry (Taniguchi et al., 2011). Our findings that VIP neurons are activated while SST neurons are inhibited during locomotion are in good agreement with the current consensus that VIP neurons mainly innervate SST neurons (Lee et al., 2013; Pfeffer et al., 2013; Pi et al., 2013), although different effects on SST neurons have also been reported (Polack et al., 2013). It has recently been shown that inhibiting SST neurons in V1 also acts to relieve surround suppression in neighboring excitatory neurons and thereby increase their visual responses (Adesnik et al., 2012), consistent with a circuit in which activating VIP neurons inhibits the activity of SST neurons to lead to increased visual response. Furthermore, besides increasing visual responses, locomotion has been shown to relieve surround suppression (Ayaz et al., 2013). SST neurons have also been found not to be active in anesthetized mice (Adesnik et al., 2012). Therefore, one would predict that activating VIP neurons in anesthetized mice would not significantly change the visual response. Indeed, although we could record strong visual responses in anesthetized mice (Figure S7C), optogenetically activating VIP neurons did not significantly change the response magnitudes (Figure S7D), a finding also consistent with a previous study (Lee et al., 2012).

Effects on stimulus selectivity are also consistent with the effects of inhibition of SST on excitatory neurons and our VIP findings. Running increases visual responses without changing stimulus selectivity (OSI) (Niell and Stryker, 2010). In the present study, activating VIP neurons increased visual responses and also did not change OSI (Figure S7A). Furthermore, activating SST neurons also suppresses the visual response without changing OSI (Lee et al., 2012). Taken together, these findings indicate that running increases visual response through activating a VIP-neuron-mediated disinhibitory circuit involving SST neurons. It has recently been shown that VIP neurons also inhibit SST neurons in prefrontal and auditory cortices and that activating VIP neurons increases auditory responses (Pi et al., 2013). Combining these with present findings suggests that VIP-neuron-mediated disinhibitory circuit is the, or at least a principal, mechanism of gain control by behavioral state in sensory cortices.

Only a small fraction of non-VIP neurons (3/77) responded to locomotion in the dark. Many or all of these were likely to be PV neurons, about half of which (24/40) were also excited in association with locomotion. However, the activity of PV neurons was not as closely coupled to locomotion as that of VIP neurons, which all responded faithfully to locomotion. The locomotion responses of many PV neurons were more transient, as evident particularly in the heterogeneous changes in their calcium signals when the animal transited from running to stationary

Figure 7. Locomotion Activates VIP Neurons in Primary Somatosensory and Auditory Cortices

(A) Example showing calcium response of a VIP neuron in barrel cortex in relation to running speed.

(B) The calcium response of VIP (red traces, n = 9, 3 mice) and non-VIP neurons (green traces, n = 15, 3 mice) in barrel cortex aligned to the running episodes (black traces). Each thin trace (red or green) is the average of all extracted responses of a single cell.

(C) Cross-correlation between calcium responses and running speed. Thin red lines show cross-correlation curves of all recorded VIP neurons. The thick red curve is the average of all thin red curves. The thick green curve is the average of the cross-correlation curves of all recorded non-VIP neurons.

(D) The average zero-time cross-correlation of VIP neurons is significantly different from that of non-VIP neurons (mean ± SEM, left, Mann-Whitney U test). The average plateau amplitude of running-aligned calcium responses is significantly different from that of non-VIP neurons (mean ± SEM, right, Mann-Whitney U test).

(E–H) Corresponding data for auditory cortex.

(Figure 3J). It has also been shown that PV neurons do not respond to ACh (Kawaguchi, 1997) and are not directly activated by stimulating basal forebrain cholinergic neurons (Alitto and Dan, 2012; Arroyo et al., 2012). The heterogeneous responses of PV neurons to locomotion are consistent with their position in the cortical circuit delineated by (Pfeffer et al., 2013). Because VIP neurons principally inhibit SST neurons, which then inhibit PV neurons, which also receive local excitation, the activity of PV neurons during locomotion would be expected to be heterogeneous, as a secondary effect of relieving the inhibition from SST neurons rather than a direct response to locomotary input. Further study is required to understand the dynamic interaction between the different classes of cortical inhibitory neurons during sensory responses. A previous study also reported that some neurons are activated during running in darkness (Keller et al., 2012). The neurons identified in that study are unlikely to be VIP neurons because they responded only briefly to some of the onsets and offsets of running, while we find that VIP neurons respond faithfully and tonically to all running episodes. It would be intriguing to identify these neurons that respond only to the onset and offset of running.

VIP neurons may be involved in other more complex circuits as well. Some VIP neurons reside in layer I or layer I/II border, and unidentified layer I interneurons have been reported to be activated by basal forebrain stimulation through nAChRs (Alitto and Dan, 2012; Letzkus et al., 2011). Activation of those layer I interneurons has been found to inhibit PV neurons and increase pyramidal neuron response in auditory cortex through this disinhibitory circuit (Letzkus et al., 2011). Since VIP neurons also target some pyramidal neurons (Alitto and Dan, 2012; Lee et al., 2012), the net physiological effect of activating VIP neurons may be more complicated than that of activating PV or SST neurons. Indeed, different interneurons might be differentially modulated by behavioral status and change the circuit function (Buia and Tiesinga, 2008).

Finally, it will be very interesting to investigate the role of VIP neurons in adult brain plasticity. While an appropriate level of inhibition is known to be important for cortical plasticity, almost all previous work on experience-dependent plasticity has focused on the role of PV neurons (Hensch, 2005). Antidepressant therapy through serotonin-reuptake inhibition has been shown to increase the capacity for ocular dominance plasticity in visual cortex in adult animals, accompanying with decreased GABA transmission (Maya Vetencourt et al., 2008). One interesting feature of VIP neurons is that they express serotonin receptor 5HT3a receptor (Lee et al., 2010; Rudy et al., 2011). Therefore, activating VIP neurons by serotonin would be expected to inhibit other inhibitory neurons and may provide a potential mechanism for effects on adult plasticity (Kuhlman et al., 2013).

EXPERIMENTAL PROCEDURES

In Vivo Two-Photon Imaging in Awake Mice

VIP, SST, and PV neurons were labeled for two-photon imaging in vivo in separate experiments by crossing tdTomato reporter mouse line with specific cre-expressing lines. Calcium imaging was performed using OGB1 or GCaMP6s in alert mice running or standing on a spherical treadmill (modified from the design of Dombeck et al., 2010). For GCaMP imaging experiment, the Cre-dependent GCaMP6s-expressing virus was injected 3 weeks before imaging experiment. Activity of identified inhibitory neuron types during stationery periods and locomotion with and without visual stimulation was compared with that of unlabeled neurons. The imaging was performed using a custom modified Movable Objective Microscope (Sutter Instrument) equipped with a femtosecond pulsed laser (Coherent) and controlled by ScanImage (http://scanimag.org). Details about mouse lines and surgery procedures could be found in the Extended Experimental Procedures.

In Vivo Tetrode Recording in Awake Mice

Extracellular microlectrode recordings were obtained using silicon microelectrodes as described previously (Niell and Stryker, 2010). Details about data acquisition and analysis could be found in the Extended Experimental Procedures.

In Vivo Drug Infusion

Inputs to VIP neurons were examined by infusion in vivo of different channel blockers using the Nanoject-II (Drummond Scientific) under the guidance of two-photon imaging. Detail procedure could be found in Extended Experimental Procedures.

Monosynaptic Retrograde Tracing

The monosynaptic connections to VIP neurons were traced using a modified rabies virus system developed by (Wickersham et al., 2007). Details of mouse lines and virus injection procedures could be found in Extended Experimental Procedures.

Optogenetic Stimulation of VIP Neurons

AAV-2/9-EF1a-DIO-ChETA-EYFP (UPenn Vector Core) was used to express ChETA in VIP neurons of VIP-Cre mice. A fiber-coupled blue LED (470 nm, Thorlabs) was used to activate ChETA-expressing neurons. Details of virus injection and photostimulation could be found in Extended Experimental Procedures.

Photo Damaging of VIP Neurons In Vivo

VIP neurons were photolytically damaged using the laser light source for two-photon imaging. Detail procedure could be found in Extended Experimental Procedures.

SUPPLEMENTAL INFORMATION

Supplemental Information includes Extended Experimental Procedures and seven figures and can be found with this article online at http://dx.doi.org/10.1016/j.cell.2014.01.050.

ACKNOWLEDGMENTS

We are grateful to Drs. Megumi Kaneko and Cristopher M. Niell for their insightful discussion and comments. This work was supported by the National Institute of Health grant EY002874 to M.P.S.

Received: July 26, 2013
Revised: November 25, 2013
Accepted: January 10, 2014
Published: February 28, 2014

REFERENCES

Adesnik, H., Bruns, W., Taniguchi, H., Huang, Z.J., and Scanziani, M. (2012). A neural circuit for spatial summation in visual cortex. Nature *490*, 226–231.

Alitto, H.J., and Dan, Y. (2012). Cell-type-specific modulation of neocortical activity by basal forebrain input. Front. Syst. Neurosci. *6*, 79.

Arroyo, S., Bennett, C., Aziz, D., Brown, S.P., and Hestrin, S. (2012). Prolonged disynaptic inhibition in the cortex mediated by slow, non-α7 nicotinic excitation of a specific subset of cortical interneurons. J. Neurosci. *32*, 3859–3864.

Ayaz, A., Saleem, A.B., Schölvinck, M.L., and Carandini, M. (2013). Locomotion controls spatial integration in mouse visual cortex. Curr. Biol. *23*, 890–894.

Bazhenov, M., Timofeev, I., Steriade, M., and Sejnowski, T.J. (2002). Model of thalamocortical slow-wave sleep oscillations and transitions to activated States. J. Neurosci. *22*, 8691–8704.

Buia, C.I., and Tiesinga, P.H. (2008). Role of interneuron diversity in the cortical microcircuit for attention. J. Neurophysiol. *99*, 2158–2182.

Chen, T.W., Wardill, T.J., Sun, Y., Pulver, S.R., Renninger, S.L., Baohan, A., Schreiter, E.R., Kerr, R.A., Orger, M.B., Jayaraman, V., et al. (2013). Ultrasensitive fluorescent proteins for imaging neuronal activity. Nature *499*, 295–300.

Chen, Y., Martinez-Conde, S., Macknik, S.L., Bereshpolova, Y., Swadlow, H.A., and Alonso, J.M. (2008). Task difficulty modulates the activity of specific neuronal populations in primary visual cortex. Nat. Neurosci. *11*, 974–982.

Crochet, S., Poulet, J.F., Kremer, Y., and Petersen, C.C. (2011). Synaptic mechanisms underlying sparse coding of active touch. Neuron *69*, 1160–1175.

Dombeck, D.A., Harvey, C.D., Tian, L., Looger, L.L., and Tank, D.W. (2010). Functional imaging of hippocampal place cells at cellular resolution during virtual navigation. Nat. Neurosci. *13*, 1433–1440.

Fontanini, A., and Katz, D.B. (2008). Behavioral states, network states, and sensory response variability. J. Neurophysiol. *100*, 1160–1168.

Gandhi, S.P., Yanagawa, Y., and Stryker, M.P. (2008). Delayed plasticity of inhibitory neurons in developing visual cortex. Proc. Natl. Acad. Sci. USA *105*, 16797–16802.

Garcia-Rill, E. (1991). The pedunculopontine nucleus. Prog. Neurobiol. *36*, 363–389.

Gentet, L.J., Kremer, Y., Taniguchi, H., Huang, Z.J., Staiger, J.F., and Petersen, C.C. (2012). Unique functional properties of somatostatin-expressing GABAergic neurons in mouse barrel cortex. Nat. Neurosci. *15*, 607–612.

Haider, B., Häusser, M., and Carandini, M. (2013). Inhibition dominates sensory responses in the awake cortex. Nature *493*, 97–100.

Harvey, C.D., Coen, P., and Tank, D.W. (2012). Choice-specific sequences in parietal cortex during a virtual-navigation decision task. Nature *484*, 62–68.

Hasselmo, M.E., and Giocomo, L.M. (2006). Cholinergic modulation of cortical function. J. Mol. Neurosci. *30*, 133–135.

Hensch, T.K. (2005). Critical period plasticity in local cortical circuits. Nat. Rev. Neurosci. *6*, 877–888.

Hill, S., and Tononi, G. (2005). Modeling sleep and wakefulness in the thalamocortical system. J. Neurophysiol. *93*, 1671–1698.

Huang, Z.J., Di Cristo, G., and Ango, F. (2007). Development of GABA innervation in the cerebral and cerebellar cortices. Nat. Rev. Neurosci. *8*, 673–686.

Huber, D., Gutnisky, D.A., Peron, S., O'Connor, D.H., Wiegert, J.S., Tian, L., Oertner, T.G., Looger, L.L., and Svoboda, K. (2012). Multiple dynamic representations in the motor cortex during sensorimotor learning. Nature *484*, 473–478.

Kawaguchi, Y. (1997). Selective cholinergic modulation of cortical GABAergic cell subtypes. J. Neurophysiol. *78*, 1743–1747.

Keller, G.B., Bonhoeffer, T., and Hübener, M. (2012). Sensorimotor mismatch signals in primary visual cortex of the behaving mouse. Neuron *74*, 809–815.

Kuhlman, S.J., Olivas, N.D., Tring, E., Ikrar, T., Xu, X., and Trachtenberg, J.T. (2013). A disinhibitory microcircuit initiates critical-period plasticity in the visual cortex. Nature *501*, 543–546.

Lee, S., Hjerling-Leffler, J., Zagha, E., Fishell, G., and Rudy, B. (2010). The largest group of superficial neocortical GABAergic interneurons expresses ionotropic serotonin receptors. J. Neurosci. *30*, 16796–16808.

Lee, S., Kruglikov, I., Huang, Z.J., Fishell, G., and Rudy, B. (2013). A disinhibitory circuit mediates motor integration in the somatosensory cortex. Nat. Neurosci. *16*, 1662–1670.

Lee, S.H., Kwan, A.C., Zhang, S., Phoumthipphavong, V., Flannery, J.G., Masmanidis, S.C., Taniguchi, H., Huang, Z.J., Zhang, F., Boyden, E.S., et al. (2012). Activation of specific interneurons improves V1 feature selectivity and visual perception. Nature *488*, 379–383.

Letzkus, J.J., Wolff, S.B., Meyer, E.M., Tovote, P., Courtin, J., Herry, C., and Lüthi, A. (2011). A disinhibitory microcircuit for associative fear learning in the auditory cortex. Nature *480*, 331–335.

Madisen, L., Zwingman, T.A., Sunkin, S.M., Oh, S.W., Zariwala, H.A., Gu, H., Ng, L.L., Palmiter, R.D., Hawrylycz, M.J., Jones, A.R., et al. (2010). A robust and high-throughput Cre reporting and characterization system for the whole mouse brain. Nat. Neurosci. *13*, 133–140.

Markram, H., Toledo-Rodriguez, M., Wang, Y., Gupta, A., Silberberg, G., and Wu, C. (2004). Interneurons of the neocortical inhibitory system. Nat. Rev. Neurosci. *5*, 793–807.

Maunsell, J.H., and Cook, E.P. (2002). The role of attention in visual processing. Philos. Trans. R. Soc. Lond. B Biol. Sci. *357*, 1063–1072.

Maya Vetencourt, J.F., Sale, A., Viegi, A., Baroncelli, L., De Pasquale, R., O'Leary, O.F., Castrén, E., and Maffei, L. (2008). The antidepressant fluoxetine restores plasticity in the adult visual cortex. Science *320*, 385–388.

Metherate, R., Cox, C.L., and Ashe, J.H. (1992). Cellular bases of neocortical activation: modulation of neural oscillations by the nucleus basalis and endogenous acetylcholine. J. Neurosci. *12*, 4701–4711.

Mink, J.W., Sinnamon, H.M., and Adams, D.B. (1983). Activity of basal forebrain neurons in the rat during motivated behaviors. Behav. Brain Res. *8*, 85–108.

Mitchell, J.F., Sundberg, K.A., and Reynolds, J.H. (2007). Differential attention-dependent response modulation across cell classes in macaque visual area V4. Neuron *55*, 131–141.

Newman, E.L., Gupta, K., Climer, J.R., Monaghan, C.K., and Hasselmo, M.E. (2012). Cholinergic modulation of cognitive processing: insights drawn from computational models. Front. Behav. Neurosci. *6*, 24.

Niell, C.M., and Stryker, M.P. (2010). Modulation of visual responses by behavioral state in mouse visual cortex. Neuron *65*, 472–479.

Petreanu, L., Gutnisky, D.A., Huber, D., Xu, N.L., O'Connor, D.H., Tian, L., Looger, L., and Svoboda, K. (2012). Activity in motor-sensory projections reveals distributed coding in somatosensation. Nature *489*, 299–303.

Pfeffer, C.K., Xue, M., He, M., Huang, Z.J., and Scanziani, M. (2013). Inhibition of inhibition in visual cortex: the logic of connections between molecularly distinct interneurons. Nat. Neurosci. *16*, 1068–1076.

Pi, H.J., Hangya, B., Kvitsiani, D., Sanders, J.I., Huang, Z.J., and Kepecs, A. (2013). Cortical interneurons that specialize in disinhibitory control. Nature *503*, 521–524.

Polack, P.O., Friedman, J., and Golshani, P. (2013). Cellular mechanisms of brain state-dependent gain modulation in visual cortex. Nat. Neurosci. *16*, 1331–1339.

Posner, M.I., and Petersen, S.E. (1990). The attention system of the human brain. Annu. Rev. Neurosci. *13*, 25–42.

Reynolds, J.H., and Chelazzi, L. (2004). Attentional modulation of visual processing. Annu. Rev. Neurosci. *27*, 611–647.

Rodriguez, R., Kallenbach, U., Singer, W., and Munk, M.H. (2004). Short- and long-term effects of cholinergic modulation on gamma oscillations and response synchronization in the visual cortex. J. Neurosci. *24*, 10369–10378.

Rudy, B., Fishell, G., Lee, S., and Hjerling-Leffler, J. (2011). Three groups of interneurons account for nearly 100% of neocortical GABAergic neurons. Dev. Neurobiol. *71*, 45–61.

Sato, H., Hata, Y., Hagihara, K., and Tsumoto, T. (1987a). Effects of cholinergic depletion on neuron activities in the cat visual cortex. J. Neurophysiol. *58*, 781–794.

Sato, H., Hata, Y., Masui, H., and Tsumoto, T. (1987b). A functional role of cholinergic innervation to neurons in the cat visual cortex. J. Neurophysiol. *58*, 765–780.

Taniguchi, H., He, M., Wu, P., Kim, S., Paik, R., Sugino, K., Kvitsiani, D., Fu, Y., Lu, J., Lin, Y., et al. (2011). A resource of Cre driver lines for genetic targeting of GABAergic neurons in cerebral cortex. Neuron *71*, 995–1013.

Weinberger, N.M. (2007). Associative representational plasticity in the auditory cortex: a synthesis of two disciplines. Learn. Mem. *14*, 1–16.

Wickersham, I.R., Lyon, D.C., Barnard, R.J., Mori, T., Finke, S., Conzelmann, K.K., Young, J.A., and Callaway, E.M. (2007). Monosynaptic restriction of transsynaptic tracing from single, genetically targeted neurons. Neuron *53*, 639–647.

Wurtz, R.H., and Mohler, C.W. (1976). Enhancement of visual responses in monkey striate cortex and frontal eye fields. J. Neurophysiol. *39*, 766–772.

Xu, N.L., Harnett, M.T., Williams, S.R., Huber, D., O'Connor, D.H., Svoboda, K., and Magee, J.C. (2012). Nonlinear dendritic integration of sensory and motor input during an active sensing task. Nature *492*, 247–251.